Functional redundancy between penicillin-binding proteins during asymmetric cell division in *Clostridioides difficile*

Shailab Shrestha[1,2†], Jules M. Dressler[1,2], Gregory A. Harrison[1], Morgan E. McNellis[1,2], & Aimee Shen[1,*]

[1]Department of Molecular Biology and Microbiology, Tufts University School of Medicine, Boston, MA, USA.

[2]Program in Molecular Microbiology, Tufts University Graduate School of Biomedical Sciences, Boston, MA, USA.

[†] Current address: Department of Microbiology, Harvard Medical School, Boston, MA, USA.

*Address correspondence to aimee.shen@tufts.edu

Abstract

Peptidoglycan synthesis is an essential driver of bacterial growth and division. The final steps of this crucial process involve the activity of the SEDS family glycosyltransferases that polymerize glycan strands and the class B penicillin-binding protein (bPBP) transpeptidases that cross-link them. While many bacteria encode multiple bPBPs to perform specialized roles during specific cellular processes, some bPBPs can play redundant roles that are important for resistance against certain cell wall stresses. Our understanding of these compensatory mechanisms, however, remains incomplete. Endospore-forming bacteria typically encode multiple bPBPs that drive morphological changes required for sporulation. The sporulation-specific bPBP, SpoVD, is important for synthesizing the asymmetric division septum and spore cortex peptidoglycan during sporulation in the pathogen *Clostridioides difficile*. Although SpoVD catalytic activity is essential for cortex synthesis, we show that it is unexpectedly dispensable for SpoVD to mediate asymmetric division. The dispensability of SpoVD's catalytic activity requires the presence of its SEDS partner, SpoVE, and is facilitated by another sporulation-induced bPBP, PBP3. Our data further suggest that PBP3 interacts with components of the asymmetric division machinery, including SpoVD. These findings suggest a possible mechanism by which bPBPs can be functionally redundant in diverse bacteria and facilitate antibiotic resistance.

28 **Importance**

29 Peptidoglycan synthesis requires the transpeptidase activity of penicillin-binding proteins
30 (PBPs), which can have specialized functions during cellular growth, division, and
31 differentiation. However, many bacteria produce PBPs with overlapping functions, and this
32 functional redundancy can increase antibiotic resistance. The spore-forming pathogen,
33 *Clostridioides difficile*, encodes four PBPs: two are essential for growth and division and
34 another, SpoVD, is essential for spore formation. Here, we show that the transpeptidase activity
35 of SpoVD is dispensable during the first morphological step of sporulation, asymmetric division,
36 because a sporulation-induced PBP, PBP3, partially substitutes for SpoVD's function during this
37 early stage. We find that SpoVD and PBP3 interact during sporulation, suggesting a mechanism
38 by which bPBPs can confer functional redundancy and potentially contribute to antibiotic
39 resistance.

Introduction

Peptidoglycan (PG) synthesis is an essential driver of the morphological changes required for bacterial growth and division. This crucial process is driven by the glycosyltransfer reactions that polymerize the glycan strands and the transpeptidation reactions that crosslink the peptide sidechains between the strands (Egan et al., 2020; Rohs & Bernhardt, 2021). These enzymatic reactions require the activities of high-molecular-weight (HMW) Penicillin-binding proteins (PBPs), which are divided into two classes based on their catalytic ability: class A PBPs (aPBP) are bifunctional enzymes capable of both glycosyltransferase and transpeptidase activities, while class B PBPs (bPBPs) are monofunctional transpeptidases (Goffin & Ghuysen, 1998; Sauvage et al., 2008). Since crosslinking of PG is essential in almost all bacteria, inhibiting PBP transpeptidase activity is typically lethal to bacterial cells. Consequently, beta-lactam antibiotics such as penicillin, which inhibit PBPs by covalently bonding to the catalytic serine residue in their transpeptidase domain, are some of the most successful and widely used antibiotics (Zapun et al., 2008). As such, identifying factors that confer resistance to beta-lactam antibiotics and determining their mechanism of action has been an area of significant interest.

One mechanism through which bacteria achieve resistance against beta-lactam antibiotics is by inducing the production of PBPs with lower binding affinities for specific beta-lactams. Most bacteria encode multiple PBPs that are specialized for specific cellular processes; some PBPs are essential, while others can be functionally redundant (Goffin & Ghuysen, 1998; Sauvage et al., 2008). Essential PBPs typically function as core components of highly conserved multiprotein complexes that drive cell wall synthesis during growth and division. The divisome is the essential complex that drives septal PG synthesis through the activities of a bPBP transpeptidase that is partnered with a cognate glycosyltransferase of the shape, elongation, division, and sporulation (SEDS) protein family (Cameron & Margolin, 2024; Rohs & Bernhardt, 2021; Taguchi et al., 2019). The elongasome is a multiprotein complex that drives cell elongation in rod-shaped bacteria through the action of a distinct SEDS-bPBP pair (Emami et al., 2017; Meeske et al., 2015; Rohs & Bernhardt, 2021; Sjodt et al., 2020). Notably, these SEDS-bPBP pairs are highly specific because the bPBP acts as a selective allosteric activator of its cognate SEDS family glycosyltransferase (Shlosman et al., 2023; Sjodt et al., 2020) (**Figure 1a**).

Endospore-forming bacteria typically encode an additional SEDS-bPBP complex that is responsible for driving the morphological changes required for spore formation (Galperin et al., 2012, 2022; Shrestha et al., 2023; Tan & Ramamurthi, 2014). Sporulation begins with the formation of a polar division septum close to one cell pole in a process called asymmetric division. In *Bacillus subtilis*, asymmetric division is driven by the same SEDS-bPBP pair that mediates cell division during vegetative growth (Muchová et al., 2020; Real et al., 2008). In contrast, we recently showed that the spore-forming pathogen *Clostridioides difficile* lacks a canonical division-associated SEDS-bPBP pair for driving septal PG synthesis and instead uses an aPBP as the major PG synthase during vegetative cell division (Shrestha et al., 2023). In further contrast with *B. subtilis,* the sporulation-specific SEDS-bPBP pair SpoVE-SpoVD is an important driver of septal PG synthesis during asymmetric division in *C. difficile*. Although the role of SpoVE-SpoVD function during asymmetric division may be restricted to *C. difficile* and other clostridial organisms, genes encoding SpoVE and SpoVD can be found in almost all spore formers (Galperin et al., 2012, 2022). In both *B. subtilis* and *C. difficile*, SpoVE and SpoVD are essential for synthesizing the spore cortex, a thick layer of modified PG that surrounds and protects the spore core (Henriques et al., 1992; Yanouri et al., 1993; Daniel et al., 1994; Shrestha et al., 2023; Alabdali et al., 2021; Srikhanta et al., 2019). Thus, SpoVE and SpoVD are important for synthesizing PG during two distinct stages of spore formation in *C. difficile*.

While a previous study showed that SpoVD's catalytic activity is essential for spore formation in *C. difficile* (Alabdali et al., 2021), in this study, we surprisingly observe that SpoVD catalytic activity is largely dispensable for mediating asymmetric division despite being essential for synthesizing the cortex layer. Prior analyses of a catalytic mutant of a divisome-associated bPBP, PBP2b$_{Bs}$, in *B. subtilis* provide a possible mechanism for explaining this observation. In *B. subtilis*, the catalytic activity of PBP2b$_{Bs}$ is dispensable because a second bPBP, PBP3$_{Bs}$, can supply the transpeptidase activity during septal PG synthesis (Sassine et al., 2017). Since the gene encoding PBP2b$_{Bs}$ is essential, presumably because the PBP2b$_{Bs}$ protein is required to allosterically activate the glycosyltransferase activity of its SEDS binding partner, FtsW, these observations highlight that PBP3$_{Bs}$ cannot complement all the roles fulfilled by the catalytically inactive PBP2b$_{Bs}$. Notably, PBP3$_{Bs}$ is also important for resistance against certain beta-lactams, since it has lower affinities for them compared to PBP2b$_{Bs}$ (Sassine et al., 2017). While these

100 observations highlight the importance of catalytic redundancies between PBPs, the molecular
101 mechanisms behind this phenomenon remain unclear.
102 Here, we explore the role of SpoVD's catalytic activity during asymmetric division in *C.*
103 *difficile*. Our findings suggest that the ability of a catalytically inactive SpoVD to support septal
104 PG synthesis during asymmetric division requires the presence of its SEDS partner SpoVE and is
105 facilitated in part by another sporulation-specific bPBP, PBP3. Furthermore, we provide evidence
106 suggesting that PBP3 interacts with components of the asymmetric division machinery, including
107 SpoVD. These findings suggest a possible mechanism for how bPBPs in diverse bacteria can be
108 functionally redundant and promote antibiotic resistance.

109 **Results**

110 **A SpoVD catalytic mutant is defective in cortex synthesis but not in asymmetric division.**

111 Given that the catalytic activity of the division-specific bPBP in *B. subtilis* is not essential
112 for its role in cell division (Sassine et al., 2017), we speculated that the catalytic activity of
113 SpoVD might be similarly dispensable during asymmetric division in *C. difficile*. SpoVD retains
114 the SXXK active-site motif that is highly conserved among bPBPs. To abolish the catalytic
115 activity of SpoVD, we introduced an alanine substitution at the nucleophilic serine residue
116 (SpoVD^{S311A}). Consistent with a prior study (Alabdali et al., 2021), *C. difficile* strains with a
117 catalytically inactive SpoVD failed to produce heat-resistant spores (**Figure S1**). Importantly,
118 this phenotype was observed when *spoVD*^{S311A} was expressed from an ectopic chromosomal
119 locus (Δ*spoVD*/*spoVD*^{S311A}) or the native locus (*spoVD*^{S311A}) (**Figure S1**).
120 To further define the role of SpoVD's catalytic activity during spore formation, we
121 evaluated the ability of the SpoVD catalytic mutant strains to progress through the different
122 morphological stages of sporulation by cytologically profiling sporulating cells (**Figures 1b** and
123 **S2**) (Nonejuie et al., 2013; Pogliano et al., 1999). Similar to the *spoVD* deletion strain, *spoVD*
124 catalytic mutant strains failed to produce phase-visible spores, indicating that they have defects
125 in cortex synthesis (**Figure 1c**). Furthermore, the distribution of sporulating cells among
126 different stages was similar between the strains, with most cells being stalled at the asymmetric
127 division stage and relatively few cells completing engulfment (**Figure 1c**). To specifically
128 quantify the effects on asymmetric division, we calculated the proportion of cells that showed

129 morphological signs of sporulation in the cytological profiling, i.e., cells that progressed beyond
130 asymmetric division, as a percentage of all cells. These analyses revealed that, relative to WT,
131 Δ*spoVD*/*spoVD*^{S311A} and *spoVD*^{S311A} cells complete asymmetric division at significantly higher
132 frequencies compared to Δ*spoVD* cells, with Δ*spoVD* cells completing asymmetric division at
133 ~30% the levels of WT and Δ*spoVD*/*spoVD*^{S311A} and *spoVD*^{S311A} cells completing asymmetric
134 division at ~70% the levels of WT (**Figure 1d**). Since we previously showed that the decreased
135 frequency of visibly sporulating Δ*spoVD* cells reflects a defect in asymmetric division rather
136 than sporulation initiation (Shrestha et al., 2023), these results suggest that SpoVD function
137 during asymmetric division is only partially dependent on its catalytic activity. Importantly, the
138 levels of SpoVD present in these strains upon sporulation induction were found to be similar to
139 wild-type (WT) by western blot analysis (**Figure 1e**).
140 Surprisingly, while we were able to complement the asymmetric division defects of the
141 catalytic mutant strains by expressing a wild-type copy of *spoVD* from an ectopic locus (**Figure**
142 **1c, 1d**), this strain was unable to form mature phase-bright spores (**Figure S1, 1c**). This suggests
143 that the catalytically inactive SpoVD has a dominant negative phenotype specifically for the
144 defect in cortex synthesis.

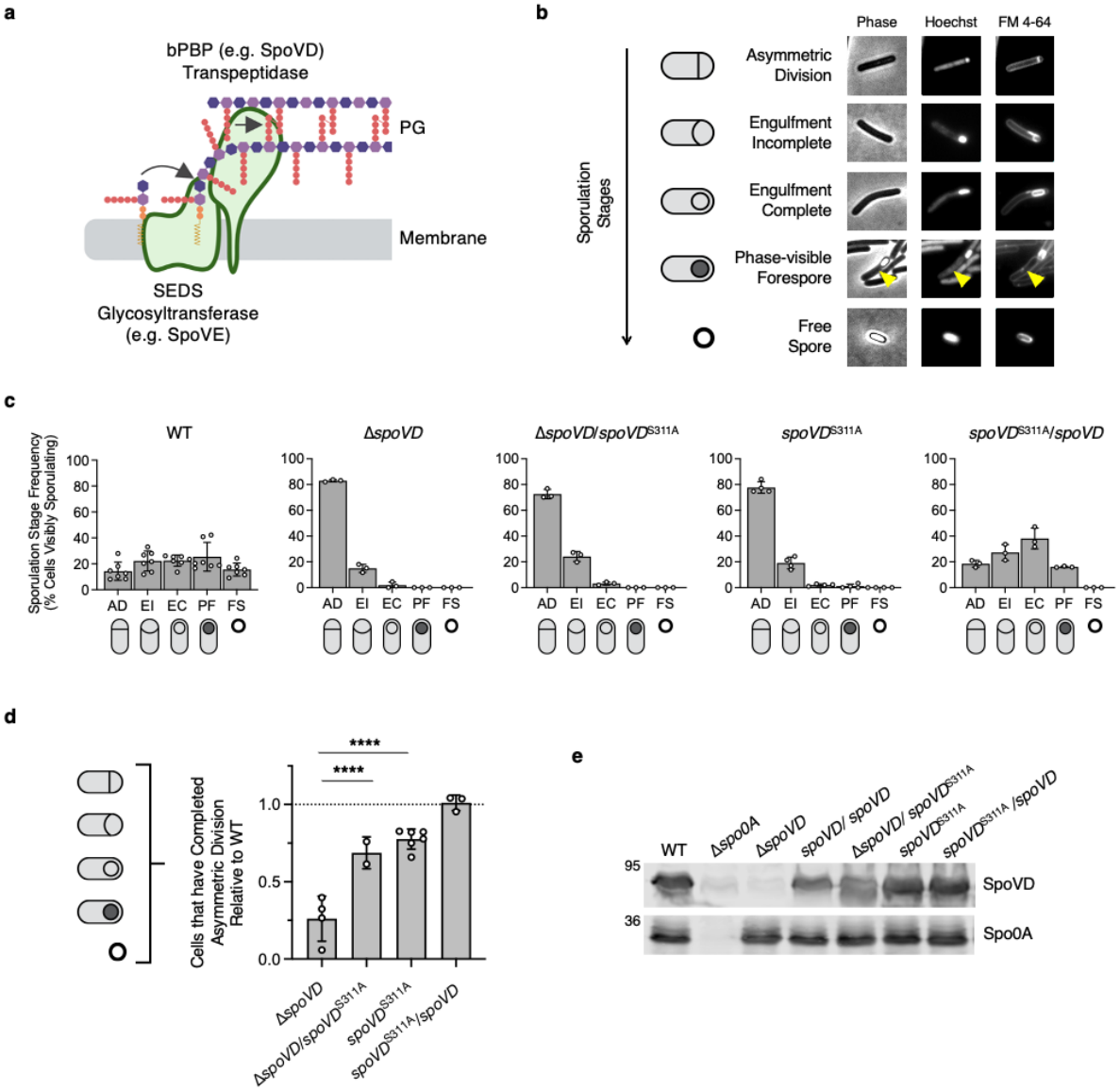

Figure 1 | SpoVD catalytic activity is partially dispensable for its function during asymmetric division. a Schematic of a SEDS-bPBP peptidoglycan synthase complex. The SEDS glycosyltransferase polymerizes nascent glycan strands from lipid-linked PG precursors in the cytoplasmic membrane, while the class B PBP (bPBP) crosslinks the stem peptides between the growing strands. **b** Cytological profile of individual cells representing each of the five morphological stages of sporulation as indicated. Representative phase-contrast and fluorescence micrographs are WT cells sampled from sporulation-inducing 70:30 plates after 18 hours of growth. The nucleoid was stained using Hoechst, and the cell membrane was stained using FM4-64. Cells undergoing asymmetric division (AD) have a flat polar septum; cells undergoing engulfment (EI) have a curved polar septum; cells that have completed engulfment (EC) are indicated by bright-membrane staining around a fully engulfed forespore; Phase-visible forespores (PF) indicate forespores completing maturation visible as phase-dark or phase-bright forespores (yellow arrow) associated with the mother cell; mature free spores (FS) are observable as independent phase-bright particles. **c, d** Quantification of the cytological profiling of cells sampled from sporulation-inducing plates after 20-22 hours of growth. White circles indicate data from each replicate, bars indicate the average means, and error bars indicate standard deviation. >1,000 total cells and >100 visibly sporulating cells per sample from a minimum of three biological replicates. **c** shows the distribution of visibly sporulating cells among the indicated stages of sporulation. **d** shows the

proportion of cells that complete and progress beyond asymmetric division, i.e., all visibly sporulating cells, as a percentage of the total cells profiled. Note that the data is normalized to WT (dotted line). **** $p < 0.0001$. Statistical significance was determined using a one-way ANOVA and Tukey's test. **e** Western blot analyses of SpoVD levels in the indicated strains 14 hours after growth on sporulation-inducing plates. The anti-Spo0A antibody was used as a proxy for measuring sporulation induction.

The SpoVD catalytic mutant requires its SEDS partner, SpoVE.

Since previous studies suggest that bPBPs are needed to allosterically activate the glycosyltransferase activity of their cognate SEDS family glycosyltransferases (Shlosman et al., 2023; Sjodt et al., 2020; Taguchi et al., 2019), we tested if the ability of SpoVD^{S311A} to support asymmetric division requires its SEDS partner SpoVE. To this end, we created a *spoVD*^{S311A}Δ*spoVE* strain by introducing the catalytic mutant variant of *spoVD* into the native locus of a Δ*spoVD*Δ*spoVE* strain. As expected, this strain failed to form heat-resistant spores (**Figure 2**). Cytological profiling of sporulating cells revealed that *spoVD*^{S311A}Δ*spoVE* cells complete and progress beyond asymmetric division at a significantly lower frequency (~25%) than WT or *spoVD*^{S311A} cells (100% and ~75%, respectively). Thus, the phenotype of *spoVD*^{S311A}Δ*spoVE* cells is similar to that of Δ*spoVD* and Δ*spoVE* cells (**Figures 1c, d & 2a, b**). Since SpoVD levels are unaffected by loss of SpoVE (**Figure 2c**), consistent with our prior results (Shrestha et al., 2023), we conclude that the function of SpoVD^{S311A} during asymmetric division requires SpoVE.

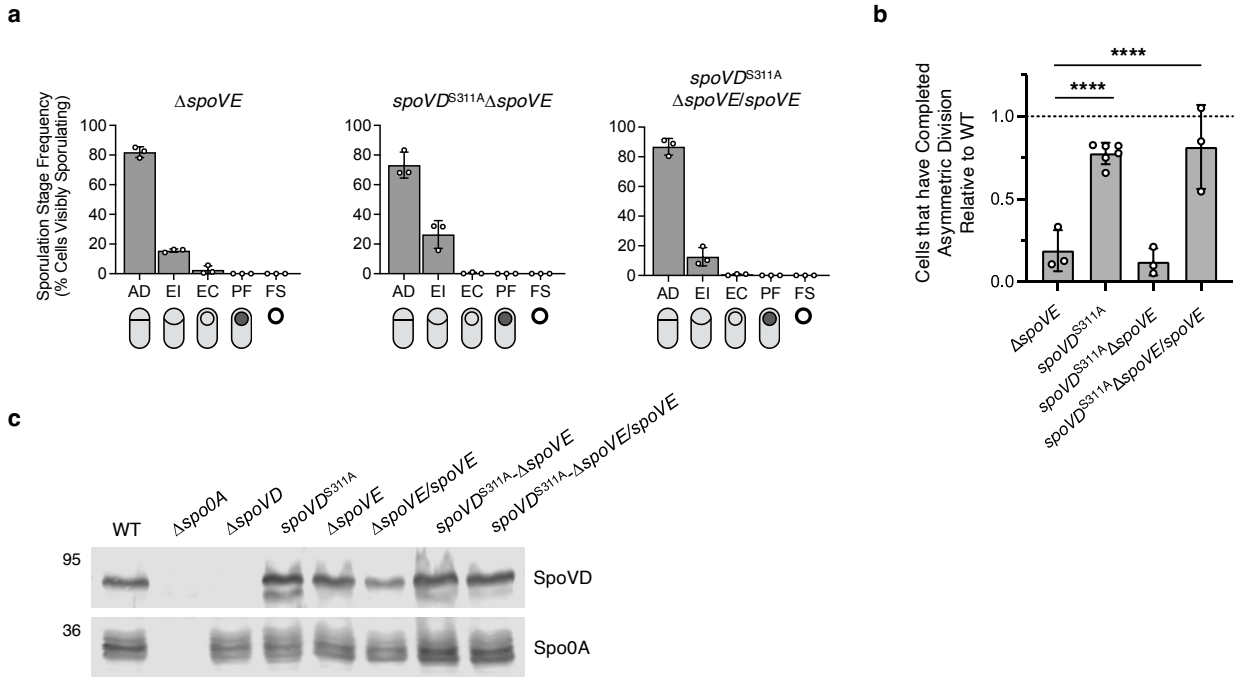

182 **Figure 2 | The catalytically inactive SpoVD requires its SEDS partner, SpoVE, to facilitate asymmetric**
183 **division. a, b** Quantification of the cytological profiling of cells sampled from sporulation-inducing plates
184 after 20-22 hours of growth. White circles indicate data from each replicate, bars indicate average means, and
185 error bars indicate standard deviation. >1,000 total cells and >100 visibly sporulating cells per sample from a
186 minimum of three biological replicates. **a** shows the distribution of visibly sporulating cells among the
187 indicated stages of sporulation. See Figure 1 for the distribution of WT cells. **b** shows the proportion of cells
188 that complete and progress beyond asymmetric division, i.e., all visibly sporulating cells, as a percentage of the
189 total cells profiled. Note that the data is normalized to WT (dotted line) and that the *spoVD*^{S311A} data derives
190 from Figure 1. *** $p < 0.001$, **** $p < 0.0001$. Statistical significance was determined using a one-way ANOVA
191 and Tukey's test. **c** Western blot analyses of SpoVD levels in the indicated strains 14 hours after growth on
192 sporulation-inducing plates. The anti-Spo0A antibody was used as a proxy for measuring sporulation
193 induction.

194 **An additional non-essential bPBP, PBP3, is involved in sporulation.**

195 Next, we wondered if *C. difficile* encodes an additional sporulation-specific bPBP that can cross-
196 link septal PG synthesis in the absence of SpoVD catalytic activity similar to the functional
197 redundancy observed between division-specific bPBPs in *B. subtilis* (Sassine et al., 2017). Most
198 *C. difficile* strains encode three bPBPs (Isidro et al., 2017, 2018): the sole essential bPBP, PBP2,
199 primarily functions during cell elongation, while the two other bPBPs, SpoVD and PBP3, are
200 dispensable for vegetative growth (Shrestha et al., 2023). PBP3 is a close homolog of SpoVD
201 containing a similar domain composition apart from the C-terminal PASTA (PBP And
202 Serine/Threonine kinase Associated) domain carried by SpoVD (**Figure 3a**). Both PBP3 and
203 SpoVD have an N-terminal transmembrane section followed by PBP dimerization and
204 transpeptidase domains.

205 We considered PBP3 to be a likely candidate for providing functional redundancy to
206 SpoVD during asymmetric division for several reasons. First, previous studies suggest that,
207 similar to *spoVD* expression, the expression of *pbp3* (locus *cd630_12290* in the strain used in
208 this study) is upregulated at the onset of sporulation (Fimlaid et al., 2013; Saujet et al., 2013).
209 Second, we previously showed that individual deletions of *spoVD* or *pbp3* do not affect the
210 growth rate of vegetative cells, suggesting that SpoVD and PBP3 play sporulation-specific roles
211 (Shrestha et al., 2023). This agrees with our western blot analysis showing that SpoVD and PBP3
212 are produced under sporulation-inducing conditions in a manner dependent on the presence of
213 the master transcriptional regulator of sporulation, Spo0A (**Figure 3b**). Taken together with prior
214 transcriptomic studies (Fimlaid et al., 2013; Saujet et al., 2013), which similarly show Spo0A-
215 dependent induction of *pbp3* and *spoVD* transcription, these observations demonstrate that both
216 proteins are produced prior to asymmetric division.

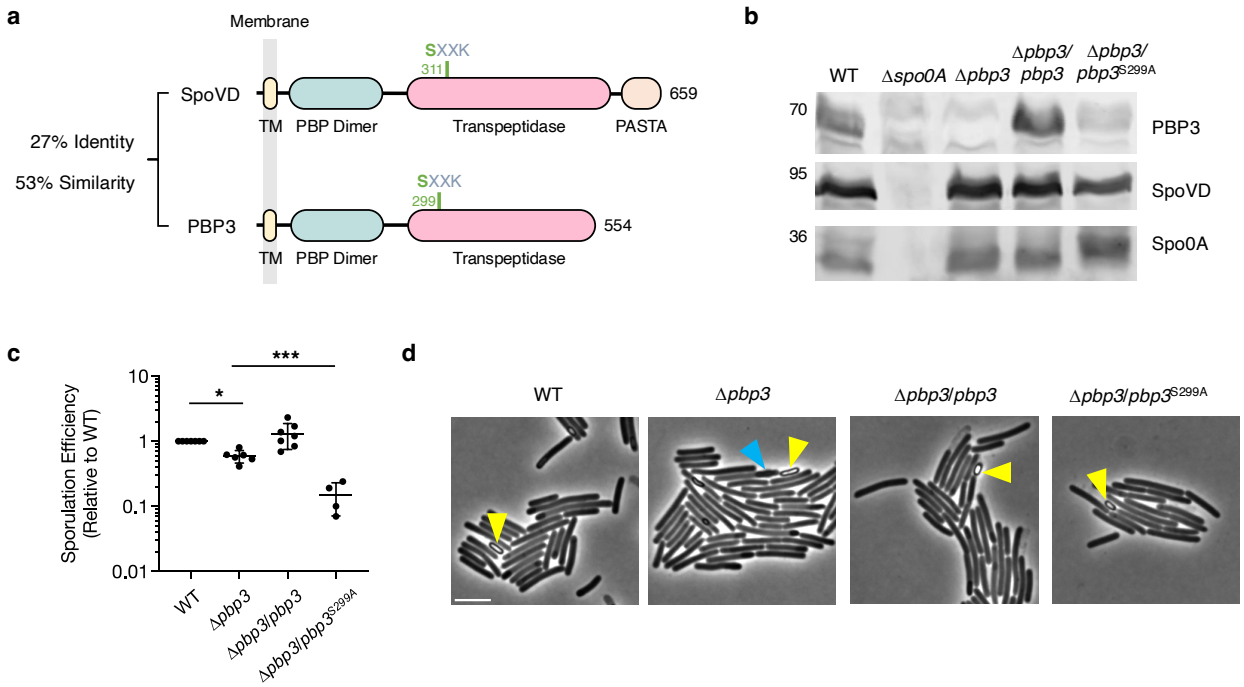

Figure 3 | PBP3 is a sporulation-specific bPBP that is involved in spore formation. a Protein schematic comparing SpoVD and PBP3. Functional domains and catalytic sites were predicted using HMMER. TM, transmembrane domain; PASTA, PBP, and serine/threonine kinase-associated domain. The catalytic serine residues are shown in green. **b** Western blot showing the levels of the SpoVD, PBP3, and Spo0A in cells sampled from sporulation-inducing plates after ~14 hours of growth. SpoVD and PBP3 are not detected in the Δ*spo0A* strain, which cannot initiate sporulation. **c** Efficiency of heat-resistant spore formation (sporulation efficiency) of the *pbp3* mutant and complemented strains relative to WT. Means with standard deviation are indicated. Cells were collected from sporulation-inducing 70:30 plates ~20-22 hours after inoculation. Data from a minimum of four biological replicates. * $p < 0.05$, *** $p < 0.001$. Statistical significance was determined using a one-way ANOVA and Tukey's test. **d** Representative phase-contrast micrographs of WT, *pbp3* mutant, and complemented cells collected from sporulation-inducing 70:30 plates after ~20 hours of growth. Examples of phase-bright spores are indicated by yellow arrows. The blue arrow highlights an elongated forespore in the Δ*pbp3* mutant. Scale bar, 5 µm.

Further characterization of the Δ*pbp3* strain revealed that it forms heat-resistant spores ~2-fold less efficiently than WT, a modest defect that can be complemented by expressing *pbp3* from an ectopic chromosomal locus (**Figure 3c**). This result is consistent with a prior transposon mutagenesis screen, which identified *pbp3* to be important for sporulation (Dembek et al., 2015). Phase-contrast microscopy of sporulating cells revealed that the Δ*pbp3* mutant forms phase-bright forespores and free spores (**Figure 3d** and **S3**), indicating that it can assemble the spore cortex unlike a Δ*spoVD* mutant. Consistent with this conclusion, transmission electron microscopy analyses detected the cortex layer in Δ*pbp3* forespores (**Figure S4**). Interestingly, these analyses also revealed that the Δ*pbp3* mutant frequently makes forespores that are

240 elongated and slightly misshapen, indicating that PBP3 affects spore formation downstream of
241 asymmetric division (**Figure S4**). The slight morphological defects may explain the reduction in
242 heat-resistant spore formation relative to WT cells. Notably, while complementation of the
243 Δ*pbp3* mutant with WT *pbp3* restored sporulation efficiency to WT levels, a strain
244 complemented with a construct encoding a catalytic mutant (*pbp3*^{S299A}) exhibited a decrease in
245 heat-resistant spore formation, indicating that PBP3's catalytic activity is important for proper
246 spore formation (**Figure 3d**). Taken together, our results indicate that PBP3 is a sporulation-
247 induced factor that is involved in, but not essential for, the formation of mature spores in *C.*
248 *difficile*.

249

250 **PBP3 promotes asymmetric division in the absence of SpoVD catalytic activity during**
251 **asymmetric division.**
252 To test if PBP3 provides redundancy to SpoVD catalytic activity during asymmetric division, we
253 analyzed the ability of Δ*pbp3* cells to complete asymmetric division in the context of WT and
254 catalytically inactive SpoVD variants. Cells lacking PBP3 completed asymmetric division at WT
255 levels in the presence of WT SpoVD (**Figure 4b**). The distribution of sporulating Δ*pbp3* cells
256 among the different sporulation stages was also similar to WT (**Figure 4a**). Importantly, in the
257 *spoVD*^{S311A} background, cells lacking PBP3 completed asymmetric division at a lower rate when
258 compared to WT or *spoVD*^{S311A} cells (**Figure 4b**). However, the proportion of *spoVD*^{S311A}Δ*pbp3*
259 cells that complete asymmetric division was higher compared to Δ*spoVD* cells (**Figure 4b**),
260 suggesting that PBP3 partially accounts for the ability of the catalytically dead SpoVD to support
261 asymmetric division. To establish if this partial redundancy requires the transpeptidase activity of
262 PBP3, we introduced *pbp3*^{S299A}, which encodes a catalytically inactive PBP3 in an ectopic
263 chromosomal locus of a *spoVD*^{S311A} Δ*pbp3* strain. Cytological profiling of the *spoVD*^{S311A}
264 Δ*pbp3*/*pbp3*^{S299A} strain revealed that these cells complete asymmetric division at levels similar to
265 WT (**Figure 4**). Hence, our data suggest that PBP3 enhances asymmetric division in the absence
266 of SpoVD catalytic activity during asymmetric division through a mechanism that is independent
267 of PBP3's transpeptidase activity.

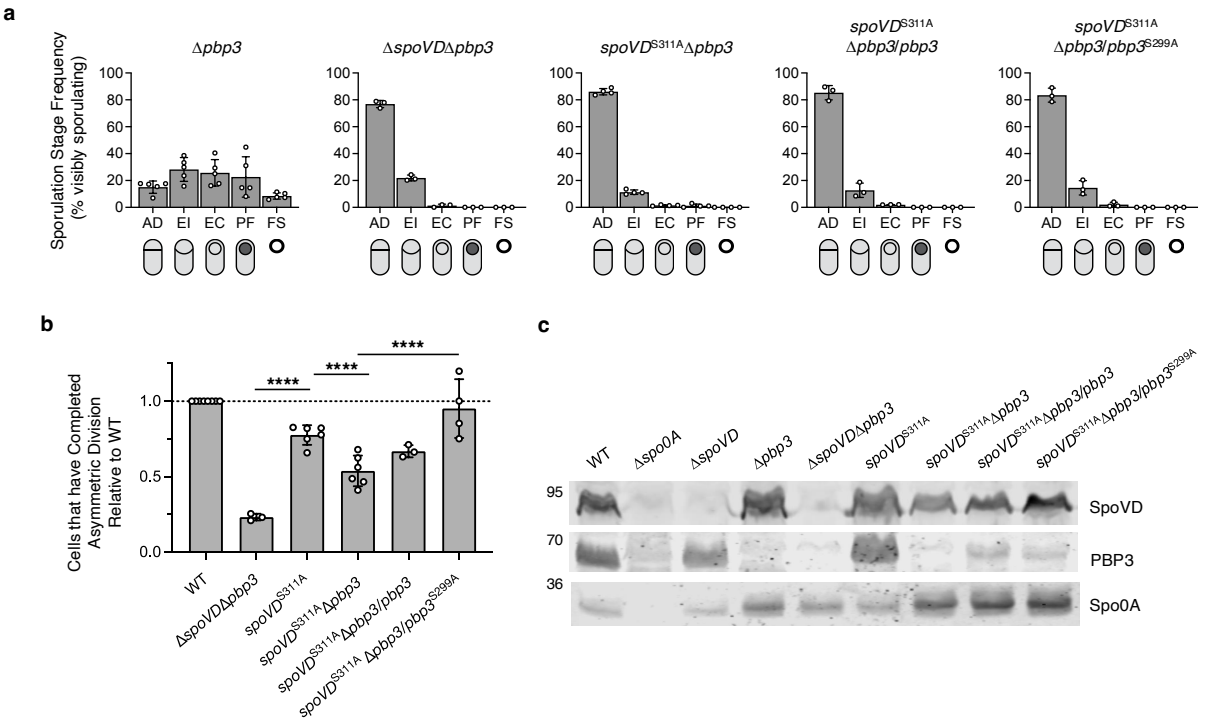

Figure 4 | PBP3 partially compensates for loss of SpoVD catalytic activity during asymmetric division. a, b Quantification of the cytological profiling of cells sampled from sporulation-inducing plates after 20-22 hours of growth. White circles indicate data from each replicate, bars indicate average means, and error bars indicate standard deviation. >1,000 total cells and >100 visibly sporulating cells per sample. Data from a minimum of three independent experiments. **** $p < 0.0001$. Statistical significance was determined using a one-way ANOVA and Tukey's test. **a** shows the distribution of visibly sporulating cells among the indicated stages of sporulation. See Figure 1b for the distribution of WT cells. **b** shows the proportion of cells that complete and progress beyond asymmetric division, i.e., all visibly sporulating cells, as a percentage of the total cells profiled. Note that the data is normalized to WT (dotted line) and that the *spoVD*^{S311A} data derives from Figure 1. **c** Western blot showing the levels of the SpoVD, PBP3, and Spo0A in cells sampled from sporulation-inducing plates after ~14 hours of growth. SpoVD and PBP3 are not detected in the Δ*spo0A* strain, which cannot initiate sporulation.

PBP3 may interact with PG-synthesizing enzymes and components of the polar divisome. Our previous study suggests that SpoVD likely functions as part of the polar divisome to synthesize septal PG during asymmetric division (Shrestha et al., 2023). The partial redundancy between PBP3 and SpoVD catalytic activities during asymmetric division observed here suggests that PBP3 might be recruited to the asymmetric division machinery during sporulation. To test whether PBP3 interacts with components of the polar divisome, we conducted bacterial two-hybrid assays to probe pairwise interactions between PBP3 and known components of this complex. In addition to SpoVD and SpoVE, we explored interactions with three additional

290 proteins, FtsL, FtsQ, and FtsB (also known as FtsL, DivIB, and DivIC in some Firmicutes),
291 which form a highly-conserved divisome sub-complex that regulates PG synthase activity during
292 cell division in other bacteria (Levin & Losick, 1994; Daniel et al., 1998; Katis & Wake, 1999;
293 Tsang & Bernhardt, 2015; Marmont & Bernhardt, 2020; Shrestha et al., 2023). Our data suggests
294 that PBP3 can interact with various components of the polar divisome, including SpoVD,
295 SpoVE, and FtsQ (**Figure 5a**). As controls, we also probed interactions between PBP3 and all
296 other PBP and SEDS-family proteins encoded by *C. difficile*. Surprisingly, our analysis indicates
297 that PBP3 also interacts with PBP2 and PBP1 (**Figure 5a**), which primarily function during
298 vegetative growth but likely also play important roles during spore formation. Although
299 surprising, PBP3 may be capable of forming a complex with all three of the other PBPs in *C.*
300 *difficile*.

301 Since bacterial two-hybrid analyses between two membrane proteins can lead to false-
302 positive results likely due to high levels of tagged proteins in the membrane non-specifically
303 reconstituting the adenylate cyclase enzyme (Yahashiri et al., 2020), we further tested whether
304 PBP3 and SpoVD interact during *C. difficile* sporulation when expressed from their native
305 promoters using co-immunoprecipitation analyses. To this end, we generated Δ*pbp3* and Δ*spoVD*
306 strains complemented with constructs encoding FLAG-tagged PBP3 and FLAG-tagged SpoVD,
307 respectively. Cell lysates were prepared from cultures grown on sporulation media for 12 hours
308 when asymmetric division peaks in sporulating cells (Oliveira et al., 2020), and the FLAG-
309 tagged PBPs were pulled-down. Western blot analyses of the pull-downs revealed that SpoVD
310 was specifically enriched in PBP3-FLAG$_3$ pull-downs (**Figure 5c**), and PBP3 was enriched in
311 SpoVD-FLAG$_3$ pull-downs (**Figure 5d**). Interestingly, PBP1, which is required for mediating
312 vegetative cell division but also likely contributes to asymmetric division (Shrestha et al., 2023),
313 was also specifically enriched in the pull-downs, suggesting that PBP1 can interact with one or
314 both SpoVD and PBP3, directly or indirectly. Importantly, a control membrane-bound
315 sporulation protein, SpoIID (Ribis et al., 2018), which is a peptidoglycan hydrolase that forms
316 part of the "engulfasome" (Kelly & Salgado, 2019), was not found in the pull-downs. Overall,
317 our data indicate that PBP3 is recruited to the polar divisome complex through direct interactions
318 with its components (**Figure 5b**).

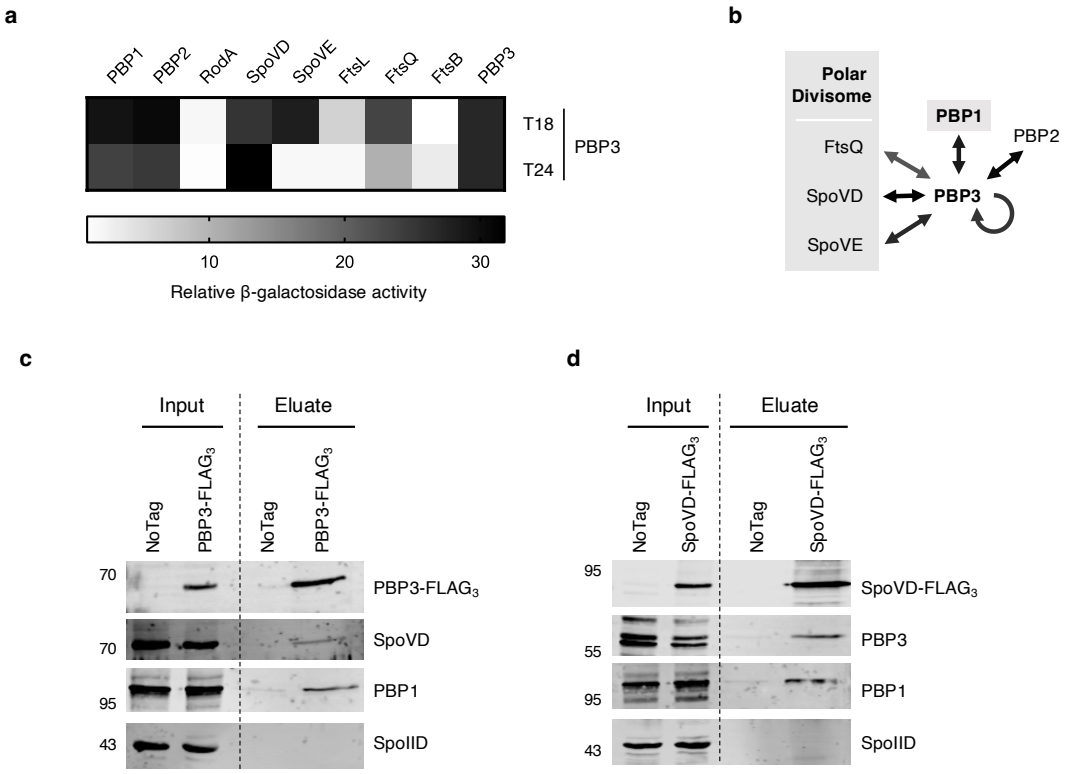

Fig. 5 | PBP3 interacts with multiple components of the polar divisome. a Bacterial two-hybrid analysis of interactions between PBP3 and other PG synthases or components of the polar divisome. The β-galactosidase activity was normalized to the negative control. N-terminal T18 or T24 fusion to PBP3 was paired with reciprocal N-terminal fusions to the indicated proteins. Data from three technical replicates. **b** The schematic shows interactions detected in the bacterial two-hybrid analyses. Components of the predicted polar divisome are indicated. PBP1 may also be a part of the polar divisome based on the co-immunoprecipitation analyses using SpoVD-FLAG$_3$ as bait. **c, d** Co-immunoprecipitations performed on cells sampled from sporulation-inducing plates after 12 hours of growth. **c** PBP3-FLAG$_3$ was used as bait in the Δ*pbp3/pbp3-FLAG$_3$* strain background; **d** SpoVD-FLAG$_3$ was used as bait in the Δ*spoVD/spoVD-FLAG$_3$* strain background. Δ*pbp3/pbp3* and Δ*spoVD/spoVD* strains were used as negative controls (No Tag). The presence of SpoVD, PBP3, and PBP1 in the pull-downs was probed using antibodies against the indicated proteins and western blotting. The FLAG-tagged proteins were detected using an anti-FLAG antibody. SpoIID was used as a control protein because it is also a PG-associated transmembrane protein localized to the forespore membrane, but it is not predicted to be a part of the polar divisome.

Endospore-forming bacteria typically encode multiple additional bPBPs compared to non-sporulating bacteria

Since *B. subtilis* also encodes multiple sporulation-specific class B PBPs, we wondered whether functional redundancies between sporulation-specific bPBPs might be more broadly conserved in endospore-forming bacteria. To this end, we compared the numbers of SEDS and bPBP enzymes

341 encoded in the genomes of non-sporulating and sporulating Firmicutes, the sole bacterial phylum
342 with endospore-forming members. Our analyses revealed that sporulating bacteria typically
343 encode a higher number of bPBPs compared to non-sporulating bacteria (**Figure 6**). In
344 sporulating organisms, the number of encoded bPBPs often exceeds the number of encoded
345 SEDS (214/328; 65%), while only a small minority encode more SEDS proteins than bPBPs
346 (20/328; 6%). Furthermore, a higher percentage of non-sporulating organisms encode equal
347 numbers of SEDS and bPBP genes (80%). These observations are consistent with the prevalence
348 of additional sporulation-specific PG synthases in spore formers and suggest that redundancy in
349 bPBP activity is likely widespread in these organisms.

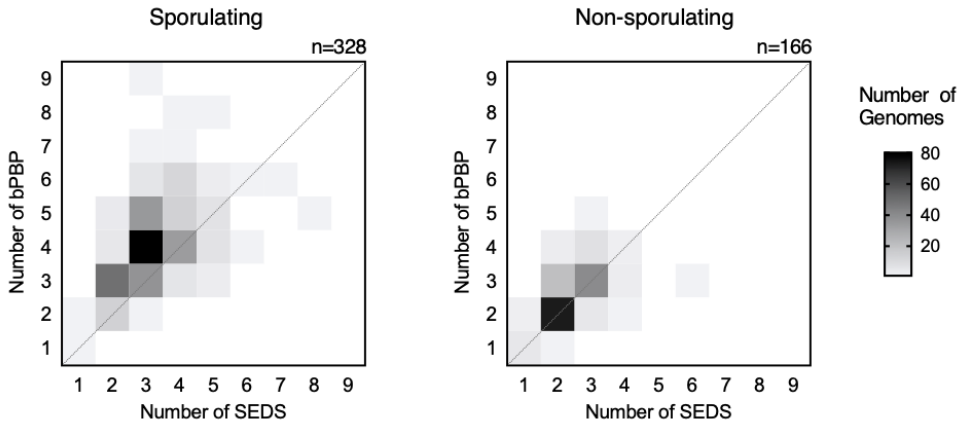

350

351 **Fig. 6 | Prevalence of bPBP and SEDS enzymes in Firmicutes.** Heatmaps showing the distribution of
352 class B penicillin-binding protein (bPBP) and SEDS protein numbers encoded in the genomes of
353 sporulating (n = 328) and non-sporulating (n = 166) Firmicutes organisms. Sporulation ability was
354 inferred by the presence of broadly conserved sporulation-specific genes *spo0A* and *spoIIE* in the
355 genome. The dataset comprises 494 diverse Firmicutes organisms, as reported in Shrestha *et al*., 2023.

356 **Discussion**

357 While most bacteria encode multiple bPBPs that perform specialized roles during specific
358 cellular processes, some bPBPs can play redundant roles that are important for resistance against
359 environmental stresses. Our understanding of these compensatory mechanisms and their
360 prevalence, however, remains incomplete. Here, we reveal that the catalytic activity of SpoVD in
361 *C. difficile* is partially dispensable for its function during the synthesis of the polar septum
362 (**Figure 1)**. Our data indicate that a previously uncharacterized sporulation-specific bPBP, PBP3,
363 partially substitutes for loss of SpoVD's catalytic activity during asymmetric division (**Figures 3,**

364 **4**), although PBP3's catalytic activity is surprisingly dispensable for promoting asymmetric
365 division in the absence of SpoVD's catalytic activity (**Figure 4**). In contrast, PBP3's catalytic
366 activity is necessary for events downstream of asymmetric division to maximize functional spore
367 formation (**Figure 3**). Finally, our bacterial two-hybrid and co-immunoprecipitation data suggest
368 that PBP3 likely functions as a part of the polar divisome, which mediates asymmetric division
369 (**Figure 5**).

370 Functional redundancies between PBPs affect the ability of bacteria to adapt to
371 environmental stresses and resist antibiotics targeting PG transpeptidation. Redundancies
372 between aPBPs have been described in *Escherichia coli* (Mueller et al., 2019), *B. subtilis,* and
373 *Streptococcus pneumoniae* (Mitchell et al., 2023), where distinct aPBPs are specialized to
374 respond to changes in environmental pH but can also play redundant roles in certain conditions.
375 Similarly, niche specialization of different bPBPs was observed in *Salmonella enterica*, which
376 encodes two division-specific and two elongation-specific bPBPs that are functionally
377 specialized for extracellular or intracellular conditions (Castanheira et al., 2017, 2020).
378 Furthermore, as described above, functional redundancy in bPBP activities during cell division in
379 *B. subtilis* lowers its sensitivity to certain beta-lactams (Sassine et al., 2017). Given that different
380 bPBPs have distinct binding affinities to beta-lactams, bPBPs that are intrinsically resistant to
381 certain beta-lactams can facilitate resistance by providing transpeptidation activity when
382 essential bPBPs are inhibited. This is supported by studies in methicillin-resistant
383 *Staphylococcus aureus* (MRSA), where strains that have acquired an additional low-affinity
384 bPBP display lower sensitivity to certain beta-lactams (Hartman & Tomasz, 1984; Wielders et
385 al., 2002). Similarly, a typically non-essential *Enterococcus faecalis* bPBP with low reactivity to
386 cephalosporins provides functional redundancy to the primary division-associated bPBP during
387 cephalosporin treatment (Djorić et al., 2020; Nelson et al., 2024).

388 While the molecular mechanisms enabling redundancies between bPBPs remain unclear,
389 these observations suggest a few possibilities. In the case of *S. enterica*, the two division-specific
390 bPBPs appear to function independently since neither bPBP requires the presence of the other to
391 function in their respective niche (Castanheira et al., 2017). Similarly, elongasome function in *B.*
392 *subtilis* can be supported by the activity of one of two distinct bPBPs, PBP2a$_{Bs}$ and PBPH$_{Bs}$ (Wei
393 et al., 2003). Notably, elongasome dynamics are unaffected in cells lacking either of the two
394 bPBPs (Middlemiss et al., 2024), so both bPBPs presumably can complex with the elongation-

395 specific SEDS protein and regulate its function. In contrast, the functional redundancy reported
396 between the division-associated bPBPs, PBP3$_{Bs}$ and PBP2b$_{Bs}$ requires the presence of the
397 catalytically inactivated PBP2b$_{Bs}$ protein (Sassine et al., 2017). Since SEDS-bPBP pairs are
398 generally thought to be comprised of cognate partners whose activities are coordinated by and
399 require their interaction (Shlosman et al., 2023; Sjodt et al., 2020; Taguchi et al., 2019), the
400 requirement of PBP2b$_{Bs}$ is likely dictated by the structural role it plays in interacting with and
401 stimulating the glycosyltransferase activity of the division-specific SEDS protein, FtsW. This is
402 consistent with an *in vitro* study, which showed that a catalytically inactive form of a bPBP can
403 support PG polymerization by its SEDS partner (Taguchi et al., 2019). Furthermore, the
404 redundancy observed in *E. faecalis* is suggested to require direct interaction between the two
405 bPBPs within the larger divisome complex (Nelson et al., 2024). In contrast, since the two
406 division-specific bPBPs in *S. enterica* can function independently from one another, it is possible
407 that either enzyme can interact with the division-specific SEDS glycosyltransferase, FtsW
408 (Castanheira et al., 2017).
409 Since the activity of *C. difficile* PBP3 during asymmetric division requires the presence
410 of SpoVD (**Figure 1**), the redundancy between the sporulation-specific SpoVD and PBP3 bPBPs
411 is more similar to the catalytic redundancy observed between division-specific bPBPs in *B.*
412 *subtilis* likely due to SpoVD allosterically activating SpoVE's activity. SpoVD may also promote
413 the formation and function of the polar divisome complex because PBP3 interacts with SpoVD
414 and potentially additional members of the polar divisome during sporulation (**Figure 5**). The
415 active recruitment of functionally redundant bPBPs to the divisome is consistent with the finding
416 that septal PG synthesis is a highly controlled process involving various localization and
417 regulatory mechanisms (Egan et al., 2020). Indeed, due to the requirement for SpoVD, we
418 speculate that PBP3 is likely recruited as an additional factor rather than replacing SpoVD in the
419 polar divisome complex. While confirmation and characterization of the mechanisms and factors
420 facilitating this recruitment require further study, our results suggest that PBP1's recruitment to
421 the polar divisome may be important for helping *spoVD* catalytic mutant strains complete
422 asymmetric division. This hypothesis is based on our observations that (i) PBP3's catalytic
423 activity is dispensable for promoting asymmetric division in a *spoVD* catalytic mutant strain
424 (**Figure 4**) and (ii) PBP1 appears to interact directly with PBP3 in two-hybrid analyses and co-

425 immunoprecipitates with both SpoVD and PBP3 purified from sporulating *C. difficile* cells
426 (**Figure 5**).
427 It remains unclear why SpoVD catalytic activity is largely dispensable during asymmetric
428 division but essential for cortex synthesis. It is possible that cortex synthesis involves SpoVE-
429 SpoVD to function as part of a larger PG synthetic complex, similar to the divisome and
430 elongasome. Since SpoVE-SpoVD function during this process requires their specific
431 localization to the forespore, it is likely that other factors are involved in their regulation. It is,
432 therefore, possible that the inability of PBP3 to functionally compensate for the loss of SpoVD
433 catalytic activity during cortex synthesis results from its decreased affinity for these unknown
434 factors. Another possibility is that the amount of crosslinking required is higher than the amount
435 PBP3 is able to supplement during this process.
436 Finally, redundancy in bPBP activity is likely widespread among spore-forming bacteria
437 based on our finding that they typically encode multiple additional bPBPs, the number of which
438 often exceeds the number of SEDS glycosyltransferases encoded in the genome (**Figure 6**).
439 Defining specialized roles or redundancies between these enzymes requires further study and
440 may have important implications for the ability of these organisms to respond to environmental
441 and antibiotic stress. Interestingly, while most *C. difficile* strains carry five distinct HMW PBPs,
442 a study characterizing clinical strains identified an additional bPBP encoded by *Clostridium*
443 *difficile* ribotype 017 isolates (Isidro et al., 2017, 2018). Some of these isolates have a lower
444 sensitivity to the beta-lactam imipenem and carry mutations in the transpeptidase catalytic sites
445 of the division-associated PBP1 and elongation-associated PBP2. The additional bPBP encoded
446 by these strains, therefore, may additionally contribute to imipenem resistance by providing
447 functional redundancy to these enzymes or SpoVD, recapitulating the scenario observed in
448 MRSA strains. Taken together with our findings, these observations highlight the need to define
449 functional redundancies between PBPs in *C. difficile* and their possible roles in driving antibiotic
450 resistance of this important pathogen.

451 **Methods**

452 *C. difficile strain construction and growth conditions*

453 All *C. difficile* strains are derived from the 630Δ*erm* strain. Deletion and complementation
454 strains were constructed in a Δ*pyrE* background strain using *pyrE*-based allele-coupled exchange
455 as previously described (Ng et al., 2013). All strains used in the study are reported in Table S1.
456 Strains were grown at 37°C under anaerobic conditions using a gas mixture containing 85% N_2,
457 5% CO_2, and 10% H_2.

458 *E. coli strain constructions*

459 Table S2 lists all plasmids used in the study, with links to plasmid maps containing all primer
460 sequences used for cloning. Plasmids were cloned via Gibson assembly, and cloned plasmids
461 were transformed into *E. coli* (DH5α or XL1-Blue strains). All plasmids were confirmed by
462 sequencing the inserted region. Confirmed plasmids were transformed into the *E. coli*
463 HB101(pRK24) strain for conjugation with *C. difficile* when needed. All *E. coli* HB101 strains
464 used for conjugation are indicated listed in Table S2.

465 *Plate-based sporulation assays*

466 For assays requiring sporulating cells, cultures were grown to early stationary phase, back-
467 diluted >25-fold into BHIS, and grown until they reached exponential phase (OD_{600} between
468 0.35 and 0.75). 120 µL of exponentially growing cells were spread onto 70:30 (70% SMC media
469 and 30% BHIS media) agar plates (40 mL media per plate). After 18-22 hours of growth,
470 sporulating cells were collected into phosphate-buffered saline (PBS), and sporulation levels
471 were visualized by phase-contrast microscopy as previously described (Pishdadian et al., 2015).

472 *Heat resistance assay*

473 Heat-resistant spore formation was measured 20-22 hours after sporulation induction on 70:30
474 agar plates by resuspending sporulating cells in PBS, dividing the sample into two, heat-treating
475 one of the samples at 60˚C for ~30 min, and comparing the colony-forming units (CFUs) in the
476 untreated sample to the heat-treated sample (Fimlaid et al., 2015). Heat-resistance efficiencies
477 represent the average ratio of heat-resistant CFUs to total CFUs for a given strain relative to the
478 average ratio for the wild-type strain.

479 *Fluorescence and phase-contrast microscopy*

480 Fluorescence microscopy was performed on sporulating cells using Hoechst 33342 (Molecular
481 Probes; 15 µg/mL) and FM4-64 (Invitrogen; 1 µg/mL) to stain nucleoid and membrane,
482 respectively. All samples for a given experiment were imaged from a single agar pad (1.5% low-
483 melting point agarose in PBS).

484 Phase-contrast images in **Figure 3** were obtained using a Zeiss Axioskop upright
485 microscope with a 100× Plan-NEOFLUAR oil-immersion phase-contrast objective and a
486 Hamamatsu C4742-95 Orca 100 CCD Camera. All other phase-contrast and fluorescence images
487 were acquired using a Leica DMi8 inverted microscope with a 63× 1.4 NA Plan Apochromat oil-
488 immersion phase-contrast objective, a high precision motorized stage (Pecon), and an incubator
489 (Pecon) set at 37˚C. Excitation light was generated by a Lumencor Spectra-X multi-LED light
490 source with integrated excitation filters. An XLED-QP quadruple-band dichroic beam-splitter
491 (Leica) was used (transmission: 415, 470, 570, and 660 nm) with an external filter wheel for all
492 fluorescent channels. FM4-464 was excited at 550/38 nm and emitted light was filtered using a
493 705/72 nm emission filter (Leica); Hoechst was excited at 395/40 nm and emitted light was
494 filtered using a 440/40 nm emission filter (Leica). Emitted and transmitted light was detected
495 using a Leica DFC 9000 GTC sCMOS camera. 1 to 2 µm z-stacks were taken when needed with
496 0.21 µm z-slices.

497 Images were acquired and exported using the LASX software without further processing.
498 After export, images were processed using Fiji (Schindelin et al., 2012) to remove out-of-focus
499 regions, and the best-focused z-planes for all channels were manually selected. Image scaling
500 was adjusted to improve brightness and contrast for display and was applied equally to all
501 images shown in a single panel. Visualization of quantified data and any associated statistical
502 tests were performed using Prism 10 (GraphPad Software, San Diego, CA, USA).

503 *Transmission electron microscopy*

504 Sporulating cells were collected ~22 h after sporulation induction on 70:30 or SMC agar plates.
505 Cells were fixed and sent for processing for electron microscopy by the University of Vermont
506 Microscopy Center, as previously described (Putnam et al., 2013; Shrestha et al., 2023). All
507 TEM images were captured on a JEOL 1400 Transmission Electron Microscope (Jeol USA, Inc.,
508 Peabody, MA) with an AMT XR611 high-resolution 11-megapixel mid-mount CCD camera.
509

510 *Western blot analysis*

511 Samples were collected 18-22 hours after sporulation induction on 70:30 agar plates and
512 processed for immunoblotting. Sample processing involved multiple freeze-thaws in PBS
513 followed by the addition of EBB buffer (9 M urea, 2 M thiourea, 4% SDS, 2 mM b-
514 mercaptoethanol), boiling, pelleting, resuspension, and boiling again before loading on a gel. All
515 proteins were resolved using 4–15% precast polyacrylamide gels (Bio-Rad) and transferred to
516 polyvinylidene difluoride membranes, which were subsequently probed with rabbit (anti-PBP3
517 (this study) and anti-SpoVD (Shrestha et al., 2023); both at 1:1,000 dilution), mouse (anti-Spo0A
518 (Fimlaid et al., 2013) at 1:1,000 dilution) and chicken (anti-GDH at 1:5,000 dilution) polyclonal
519 primary antibodies, and anti-rabbit (IR800 or IR680), anti-mouse (IR680) and anti-chicken
520 (IR800) secondary antibodies (LI-COR Biosciences, 1:20,000 dilution). Blots were imaged using
521 a LiCor Odyssey CLx imaging system. The results shown are representative of multiple
522 experiments.

523 *Antibody production*

524 Anti-PBP3 and anti-PBP1 antibodies used for western blots in this study were raised in rabbits
525 by Cocalico Biologicals against PBP3 and PBP1 variants lacking the transmembrane domains.
526 PBP3$_{\Delta 1\text{-}35}$-His$_6$ and His$_6$-PBP1$_{\Delta 1\text{-}77}$ were produced in BL21(DE3) *E. coli* harboring pET28a-*pbp3*
527 $_{\Delta 1\text{-}35}$-His$_6$ and pET28a-His$_6$-*pbp1*$_{\Delta 1\text{-}77}$, respectively, and purified by Ni^{2+}-affinity purification as
528 previously described (Fimlaid et al., 2013). Antisera reactivity and specificity for PBP3 and
529 PBP1 were validated by western blot against *C. difficile* lysate from WT and either a Δ*pbp3*
530 mutant (this work) or a *pbp1* CRISPR-interference knock-down strain (Shrestha et al., 2023),
531 respectively.

532 *Bacterial two-hybrid analyses*

533 Bacterial adenylate cyclase two-hybrid (BACTH) assays were conducted as previously described
534 (Karimova et al., 1998) using *E. coli* BTH101 cells. Briefly, BTH101 cells were transformed
535 with 100 ng of each plasmid and plated on LB agar plates supplemented with 50 µg/ml
536 kanamycin, 100 µg/ml Ampicillin, and 0.5 mM isopropyl β-D-thiogalactopyranoside (IPTG).
537 Plates were incubated for 64-68 hours at 30°C, and β-galactosidase activity was quantified in
538 Miller units as previously detailed (Dahlstrom et al., 2015). The β-galactosidase activity of cells

539 transformed with the empty pUT18C and pKT25 vectors was used as a negative control for
540 normalization.

541 *Co-immunoprecipitation (Co-IP) analyses*

542 To immunoprecipitate FLAG-tagged proteins from sporulating *C. difficile*, exponentially
543 growing cultures of *C. difficile* harboring pbp3-FLAG3 or spoVD-FLAG3 expression constructs
544 and appropriate control strains were spread onto 70:30 agar plates. After 12 hours of growth on
545 70:30 plates, sporulating cells were scraped from 3 plates per strain and pooled in 1 mL of PBS.
546 A portion of cells was visualized by microscopy with peptidoglycan labeling to confirm the
547 presence of sporulating cells undergoing asymmetric division in each sample. Cells were
548 crosslinked with 0.25% final concentration of PFA for 15 minutes at 37°C and quenched with
549 350 mM glycine for 10 minutes on ice. Crosslinked cells were then pelleted, re-suspended in 750
550 µL of FLAG IP Buffer (150 mM NaCl, 50 mM Tris-HCl pH 7.5), transferred to screwcap tubes
551 containing MP Biomedicals Lysing Matrix E, and frozen at -80°C. Frozen cells were thawed and
552 bead beat on an MP Biomedicals FastPrep-24 four times at 5.5 M/second for 1 minute, resting on
553 ice for 5 minutes between rounds of bead-beating. Next, 1X HALT protease inhibitors and
554 dodecyl-β-d-maltoside (DDM) detergent were added to lysed cells to a final concentration of
555 0.5%, and mixtures were rotated at room temperature for 1 hour to solubilize membrane proteins.
556 Lysates were clarified by centrifuging at 10,000 × g for 1 minute, and 200 µL of pre-equilibrated
557 Anti-FLAG M2 Magnetic Dynabead resin was added to the clarified lysate. The lysate-resin
558 mixture was rotated at room temperature for 1 hour. To remove unbound proteins, the resin was
559 washed three times briefly and once for 5 minutes with 1 mL FLAG IP Buffer containing 0.5%
560 DDM. Then, the resin was washed three times briefly and once for 5 minutes with FLAG IP
561 Buffer containing no detergent. This step was repeated a total of two times. Finally, bound
562 proteins were eluted from the resin with 2 µg/mL 3XFLAG peptide, boiled in 1X sample buffer
563 for 10 minutes to reverse crosslinks, and then analyzed by western blot using rabbit polyclonal
564 antibodies against PBP1 (TF134, this study), PBP3 (TF135, this study), SpoVD (TF124,
565 (Shrestha et al., 2023)), SpoIID (TF121, (Ribis et al., 2018)), or a mouse monoclonal M2 anti-
566 FLAG antibody (Sigma).

Acknowledgments

We acknowledge the University of Vermont Microscopy Imaging Core for processing the samples and acquiring the images for all Transmission Electron Microscopy analyses. We are grateful to members of the Shen lab for helpful discussions and feedback on the project. The National Institute of Allergy and Infectious Diseases grant R01 AI122232 (to A.S.) and Burroughs Wellcome Fund for Investigators in Pathogenesis Award (to A.S.) provided funding for this work. Additionally, G.A.H. was supported by the Tufts University Institutional Research Career and Academic Development Award Program funded by the National Institute of General Medical Sciences K12 GM133314.

Author Contributions

S.S. and A.S. conceived the study. S.S., J.M.D., G.A.H., M.M, and A.S. performed and analyzed experiments. A.S. supervised the study. S.S. and A.S. wrote the manuscript with input from the other authors. All authors reviewed and approved the manuscript.

580 **References**

581 Alabdali, Y. A. J., Oatley, P., Kirk, J. A., & Fagan, R. P. (2021). A cortex-specific penicillin-
582 binding protein contributes to heat resistance in Clostridioides difficile spores. *Anaerobe*,
583 *70*, 102379. https://doi.org/10.1016/j.anaerobe.2021.102379
584 Cameron, T. A., & Margolin, W. (2024). Insights into the assembly and regulation of the bacterial
585 divisome. *Nature Reviews Microbiology*, *22*(1), 33–45. https://doi.org/10.1038/s41579-
586 023-00942-x
587 Castanheira, S., Cestero, J. J., Rico-Pérez, G., García, P., Cava, F., Ayala, J. A., Pucciarelli, M.
588 G., & García-del Portillo, F. (2017). A Specialized Peptidoglycan Synthase Promotes
589 *Salmonella* Cell Division inside Host Cells. *mBio*, *8*(6), e01685-17.
590 https://doi.org/10.1128/mBio.01685-17
591 Castanheira, S., López-Escarpa, D., Pucciarelli, M. G., Cestero, J. J., Baquero, F., & García-del
592 Portillo, F. (2020). An alternative penicillin-binding protein involved in Salmonella
593 relapses following ceftriaxone therapy. *eBioMedicine*, *55*, 102771.
594 https://doi.org/10.1016/j.ebiom.2020.102771
595 Dahlstrom, K. M., Giglio, K. M., Collins, A. J., Sondermann, H., & O'Toole, G. A. (2015).
596 Contribution of Physical Interactions to Signaling Specificity between a Diguanylate
597 Cyclase and Its Effector. *mBio*, *6*(6), 10.1128/mbio.01978-15.
598 https://doi.org/10.1128/mbio.01978-15
599 Daniel, R. A., Drake, S., Buchanan, C. E., Scholle, R., & Errington, J. (1994). The Bacillus
600 subtilis spoVD gene encodes a mother-cell-specific penicillin-binding protein required
601 for spore morphogenesis. *Journal of Molecular Biology*, *235*(1), 209–220.
602 https://doi.org/10.1016/S0022-2836(05)80027-0
603 Daniel, R. A., Harry, E. J., Katis, V. L., Wake, R. G., & Errington, J. (1998). Characterization of
604 the essential cell division gene ftsL(yIID) of Bacillus subtilis and its role in the assembly
605 of the division apparatus. *Molecular Microbiology*, *29*(2), 593–604.
606 https://doi.org/10.1046/j.1365-2958.1998.00954.x
607 Dembek, M., Barquist, L., Boinett, C. J., Cain, A. K., Mayho, M., Lawley, T. D., Fairweather, N.
608 F., & Fagan, R. P. (2015). High-throughput analysis of gene essentiality and sporulation
609 in Clostridium difficile. *mBio*, *6*(2), e02383. https://doi.org/10.1128/mBio.02383-14

610 Djorić, D., Little, J. L., & Kristich, C. J. (2020). Multiple Low-Reactivity Class B Penicillin-
611 Binding Proteins Are Required for Cephalosporin Resistance in Enterococci.
612 *Antimicrobial Agents and Chemotherapy*, *64*(4), 10.1128/aac.02273-19.
613 https://doi.org/10.1128/aac.02273-19
614 Egan, A. J. F., Errington, J., & Vollmer, W. (2020). Regulation of peptidoglycan synthesis and
615 remodelling. *Nature Reviews. Microbiology*, *18*(8), 446–460.
616 https://doi.org/10.1038/s41579-020-0366-3
617 Emami, K., Guyet, A., Kawai, Y., Devi, J., Wu, L. J., Allenby, N., Daniel, R. A., & Errington, J.
618 (2017). RodA as the missing glycosyltransferase in Bacillus subtilis and antibiotic
619 discovery for the peptidoglycan polymerase pathway. *Nature Microbiology*, *2*, 16253.
620 https://doi.org/10.1038/nmicrobiol.2016.253
621 Fimlaid, K. A., Bond, J. P., Schutz, K. C., Putnam, E. E., Leung, J. M., Lawley, T. D., & Shen, A.
622 (2013). Global Analysis of the Sporulation Pathway of Clostridium difficile. *PLoS*
623 *Genetics*, *9*(8), e1003660. https://doi.org/10.1371/journal.pgen.1003660
624 Fimlaid, K. A., Jensen, O., Donnelly, M. L., Francis, M. B., Sorg, J. A., & Shen, A. (2015).
625 Identification of a Novel Lipoprotein Regulator of Clostridium difficile Spore
626 Germination. *PLOS Pathogens*, *11*(10), e1005239.
627 https://doi.org/10.1371/journal.ppat.1005239
628 Galperin, M. Y., Mekhedov, S. L., Puigbo, P., Smirnov, S., Wolf, Y. I., & Rigden, D. J. (2012).
629 Genomic determinants of sporulation in Bacilli and Clostridia: Towards the minimal set
630 of sporulation-specific genes. *Environmental Microbiology*, *14*(11), 2870–2890.
631 https://doi.org/10.1111/j.1462-2920.2012.02841.x
632 Galperin, M. Y., Yutin, N., Wolf, Y. I., Vera Alvarez, R., & Koonin, E. V. (2022). Conservation
633 and Evolution of the Sporulation Gene Set in Diverse Members of the Firmicutes.
634 *Journal of Bacteriology*, *204*(6), e00079-22. https://doi.org/10.1128/jb.00079-22
635 Goffin, C., & Ghuysen, J.-M. (1998). Multimodular Penicillin-Binding Proteins: An Enigmatic
636 Family of Orthologs and Paralogs. *Microbiology and Molecular Biology Reviews*, *62*(4),
637 1079–1093.
638 Hartman, B. J., & Tomasz, A. (1984). Low-affinity penicillin-binding protein associated with
639 beta-lactam resistance in Staphylococcus aureus. *Journal of Bacteriology*, *158*(2), 513–
640 516. https://doi.org/10.1128/jb.158.2.513-516.1984

641 Henriques, A. O., de Lencastre, H., & Piggot, P. J. (1992). A Bacillus subtilis morphogene cluster
642 that includes spoVE is homologous to the mra region of Escherichia coli. *Biochimie*,
643 *74*(7–8), 735–748. https://doi.org/10.1016/0300-9084(92)90146-6
644 Isidro, J., Mendes, A. L., Serrano, M., O.Henriques, A., & Oleastro, M. (2017). Overview of
645 Clostridium difficile Infection: Life Cycle, Epidemiology, Antimicrobial Resistance and
646 Treatment. *Clostridium Difficile - A Comprehensive Overview*.
647 https://doi.org/10.5772/intechopen.69053
648 Isidro, J., Santos, A., Nunes, A., Borges, V., Silva, C., Vieira, L., Mendes, A. L., Serrano, M.,
649 Henriques, A. O., Gomes, J. P., & Oleastro, M. (2018). Imipenem Resistance in
650 *Clostridium difficile* Ribotype 017, Portugal. *Emerging Infectious Diseases*, *24*(4), 741–
651 745. https://doi.org/10.3201/eid2404.170095
652 Karimova, G., Pidoux, J., Ullmann, A., & Ladant, D. (1998). A bacterial two-hybrid system
653 based on a reconstituted signal transduction pathway. *Proceedings of the National*
654 *Academy of Sciences*, *95*(10), 5752–5756. https://doi.org/10.1073/pnas.95.10.5752
655 Katis, V. L., & Wake, R. G. (1999). Membrane-bound division proteins DivIB and DivIC of
656 Bacillus subtilis function solely through their external domains in both vegetative and
657 sporulation division. *Journal of Bacteriology*, *181*(9), 2710–2718.
658 https://doi.org/10.1128/JB.181.9.2710-2718.1999
659 Kelly, A., & Salgado, P. S. (2019). The engulfasome in C. difficile: Variations on protein
660 machineries. *Anaerobe*, *60*, 102091. https://doi.org/10.1016/j.anaerobe.2019.102091
661 Levin, P. A., & Losick, R. (1994). Characterization of a cell division gene from Bacillus subtilis
662 that is required for vegetative and sporulation septum formation. *Journal of Bacteriology*,
663 *176*(5), 1451–1459. https://doi.org/10.1128/jb.176.5.1451-1459.1994
664 Marmont, L. S., & Bernhardt, T. G. (2020). A conserved subcomplex within the bacterial
665 cytokinetic ring activates cell wall synthesis by the FtsW-FtsI synthase. *Proceedings of*
666 *the National Academy of Sciences*, *117*(38), 23879–23885.
667 https://doi.org/10.1073/pnas.2004598117
668 Meeske, A. J., Sham, L.-T., Kimsey, H., Koo, B.-M., Gross, C. A., Bernhardt, T. G., & Rudner,
669 D. Z. (2015). MurJ and a novel lipid II flippase are required for cell wall biogenesis in
670 Bacillus subtilis. *Proceedings of the National Academy of Sciences*, *112*(20), 6437–6442.
671 https://doi.org/10.1073/pnas.1504967112

672 Middlemiss, S., Blandenet, M., Roberts, D. M., McMahon, A., Grimshaw, J., Edwards, J. M.,
673 Sun, Z., Whitley, K. D., Blu, T., Strahl, H., & Holden, S. (2024). Molecular motor tug-of-
674 war regulates elongasome cell wall synthesis dynamics in Bacillus subtilis. *Nature*
675 *Communications*, *15*(1), 5411. https://doi.org/10.1038/s41467-024-49785-x
676 Mitchell, S. L., Kearns, D. B., & Carlson, E. E. (2023). Penicillin-binding protein redundancy in
677 Bacillus subtilis enables growth during alkaline shock. *bioRxiv*, 2023.03.20.533529.
678 https://doi.org/10.1101/2023.03.20.533529
679 Muchová, K., Chromiková, Z., & Barák, I. (2020). Linking the Peptidoglycan Synthesis Protein
680 Complex with Asymmetric Cell Division during Bacillus subtilis Sporulation.
681 *International Journal of Molecular Sciences*, *21*(12), 4513.
682 https://doi.org/10.3390/ijms21124513
683 Mueller, E. A., Egan, A. J., Breukink, E., Vollmer, W., & Levin, P. A. (2019). Plasticity of
684 Escherichia coli cell wall metabolism promotes fitness and antibiotic resistance across
685 environmental conditions. *eLife*, *8*, e40754. https://doi.org/10.7554/eLife.40754
686 Nelson, M. E., Little, J. L., & Kristich, C. J. (2024). Pbp4 provides transpeptidase activity to the
687 FtsW-PbpB peptidoglycan synthase to drive cephalosporin resistance in Enterococcus
688 faecalis. *Antimicrobial Agents and Chemotherapy*, *68*(9), e00555-24.
689 https://doi.org/10.1128/aac.00555-24
690 Ng, Y. K., Ehsaan, M., Philip, S., Collery, M. M., Janoir, C., Collignon, A., Cartman, S. T., &
691 Minton, N. P. (2013). Expanding the Repertoire of Gene Tools for Precise Manipulation
692 of the Clostridium difficile Genome: Allelic Exchange Using pyrE Alleles. *PLOS ONE*,
693 *8*(2), e56051. https://doi.org/10.1371/journal.pone.0056051
694 Nonejuie, P., Burkart, M., Pogliano, K., & Pogliano, J. (2013). Bacterial cytological profiling
695 rapidly identifies the cellular pathways targeted by antibacterial molecules. *Proceedings*
696 *of the National Academy of Sciences*, *110*(40), 16169–16174.
697 https://doi.org/10.1073/pnas.1311066110
698 Oliveira, P. H., Ribis, J. W., Garrett, E. M., Trzilova, D., Kim, A., Sekulovic, O., Mead, E. A.,
699 Pak, T., Zhu, S., Deikus, G., Touchon, M., Lewis-Sandari, M., Beckford, C., Zeitouni, N.
700 E., Altman, D. R., Webster, E., Oussenko, I., Bunyavanich, S., Aggarwal, A. K., … Fang,
701 G. (2020). Epigenomic characterization of Clostridioides difficile finds a conserved DNA

methyltransferase that mediates sporulation and pathogenesis. *Nature Microbiology*, *5*(1), Article 1. https://doi.org/10.1038/s41564-019-0613-4

Pishdadian, K., Fimlaid, K. A., & Shen, A. (2015). SpoIIID-mediated regulation of σK function during Clostridium difficile sporulation. *Molecular Microbiology*, *95*(2), 189–208. https://doi.org/10.1111/mmi.12856

Pogliano, J., Osborne, N., Sharp, M. D., Abanes-De Mello, A., Perez, A., Sun, Y.-L., & Pogliano, K. (1999). A vital stain for studying membrane dynamics in bacteria: A novel mechanism controlling septation during Bacillus subtilis sporulation. *Molecular Microbiology*, *31*(4), 1149–1159. https://doi.org/10.1046/j.1365-2958.1999.01255.x

Putnam, E. E., Nock, A. M., Lawley, T. D., & Shen, A. (2013). SpoIVA and SipL Are Clostridium difficile Spore Morphogenetic Proteins. *Journal of Bacteriology*, *195*(6), 1214–1225. https://doi.org/10.1128/JB.02181-12

Real, G., Fay, A., Eldar, A., Pinto, S. M., Henriques, A. O., & Dworkin, J. (2008). Determinants for the Subcellular Localization and Function of a Nonessential SEDS Protein. *Journal of Bacteriology*, *190*(1), 363–376. https://doi.org/10.1128/jb.01482-07

Ribis, J. W., Fimlaid, K. A., & Shen, A. (2018). Differential requirements for conserved peptidoglycan remodeling enzymes during Clostridioides difficile spore formation. *Molecular Microbiology*, *110*(3), 370–389. https://doi.org/10.1111/mmi.14090

Rohs, P. D. A., & Bernhardt, T. G. (2021). Growth and Division of the Peptidoglycan Matrix. *Annual Review of Microbiology*, *75*(1), 315–336. https://doi.org/10.1146/annurev-micro-020518-120056

Sassine, J., Xu, M., Sidiq, K. R., Emmins, R., Errington, J., & Daniel, R. A. (2017). Functional redundancy of division specific penicillin-binding proteins in Bacillus subtilis. *Molecular Microbiology*, *106*(2), 304–318. https://doi.org/10.1111/mmi.13765

Saujet, L., Pereira, F. C., Serrano, M., Soutourina, O., Monot, M., Shelyakin, P. V., Gelfand, M. S., Dupuy, B., Henriques, A. O., & Martin-Verstraete, I. (2013). Genome-wide analysis of cell type-specific gene transcription during spore formation in Clostridium difficile. *PLoS Genetics*, *9*(10), e1003756. https://doi.org/10.1371/journal.pgen.1003756

Sauvage, E., Kerff, F., Terrak, M., Ayala, J. A., & Charlier, P. (2008). The penicillin-binding proteins: Structure and role in peptidoglycan biosynthesis. *FEMS Microbiology Reviews*, *32*(2), 234–258. https://doi.org/10.1111/j.1574-6976.2008.00105.x

733 Schindelin, J., Arganda-Carreras, I., Frise, E., Kaynig, V., Longair, M., Pietzsch, T., Preibisch, S.,
734 Rueden, C., Saalfeld, S., Schmid, B., Tinevez, J.-Y., White, D. J., Hartenstein, V., Eliceiri,
735 K., Tomancak, P., & Cardona, A. (2012). Fiji: An open-source platform for biological-
736 image analysis. *Nature Methods*, *9*(7), Article 7. https://doi.org/10.1038/nmeth.2019
737 Shlosman, I., Fivenson, E. M., Gilman, M. S. A., Sisley, T. A., Walker, S., Bernhardt, T. G.,
738 Kruse, A. C., & Loparo, J. J. (2023). Allosteric activation of cell wall synthesis during
739 bacterial growth. *Nature Communications*, *14*(1), Article 1.
740 https://doi.org/10.1038/s41467-023-39037-9
741 Shrestha, S., Taib, N., Gribaldo, S., & Shen, A. (2023). Diversification of division mechanisms in
742 endospore-forming bacteria revealed by analyses of peptidoglycan synthesis in
743 Clostridioides difficile. *Nature Communications*, *14*(1), 7975.
744 https://doi.org/10.1038/s41467-023-43595-3
745 Sjodt, M., Rohs, P. D. A., Gilman, M. S. A., Erlandson, S. C., Zheng, S., Green, A. G., Brock, K.
746 P., Taguchi, A., Kahne, D., Walker, S., Marks, D. S., Rudner, D. Z., Bernhardt, T. G., &
747 Kruse, A. C. (2020). Structural coordination of polymerization and crosslinking by a
748 SEDS–bPBP peptidoglycan synthase complex. *Nature Microbiology*, *5*(6), Article 6.
749 https://doi.org/10.1038/s41564-020-0687-z
750 Srikhanta, Y. N., Hutton, M. L., Awad, M. M., Drinkwater, N., Singleton, J., Day, S. L.,
751 Cunningham, B. A., McGowan, S., & Lyras, D. (2019). Cephamycins inhibit pathogen
752 sporulation and effectively treat recurrent Clostridioides difficile infection. *Nature*
753 *Microbiology*, *4*(12), 2237–2245. https://doi.org/10.1038/s41564-019-0519-1
754 Taguchi, A., Welsh, M. A., Marmont, L. S., Lee, W., Sjodt, M., Kruse, A. C., Kahne, D.,
755 Bernhardt, T. G., & Walker, S. (2019). FtsW is a peptidoglycan polymerase that is
756 functional only in complex with its cognate penicillin-binding protein. *Nature*
757 *Microbiology*, *4*(4), Article 4. https://doi.org/10.1038/s41564-018-0345-x
758 Tan, I. S., & Ramamurthi, K. S. (2014). Spore formation in Bacillus subtilis. *Environmental*
759 *Microbiology Reports*, *6*(3), 212–225. https://doi.org/10.1111/1758-2229.12130
760 Tsang, M.-J., & Bernhardt, T. G. (2015). A role for the FtsQLB complex in cytokinetic ring
761 activation revealed by an ftsL allele that accelerates division. *Molecular Microbiology*,
762 *95*(6), 925–944. https://doi.org/10.1111/mmi.12905

763 Wei, Y., Havasy, T., McPherson, D. C., & Popham, D. L. (2003). Rod Shape Determination by
764 the Bacillus subtilis Class B Penicillin-Binding Proteins Encoded by pbpA and pbpH.
765 *Journal of Bacteriology*, *185*(16), 4717–4726. https://doi.org/10.1128/jb.185.16.4717-
766 4726.2003
767 Wielders, C. L. C., Fluit, A. C., Brisse, S., Verhoef, J., & Schmitz, F. J. (2002). *mecA* Gene Is
768 Widely Disseminated in *Staphylococcus aureus* Population. *Journal of Clinical*
769 *Microbiology*, *40*(11), 3970–3975. https://doi.org/10.1128/JCM.40.11.3970-3975.2002
770 Yahashiri, A., Babor, J. T., Anwar, A. L., Bezy, R. P., Piette, E. W., Arends, S. J. R., Müh, U.,
771 Steffen, M. R., Cline, J. M., Stanek, D. N., Lister, S. D., Swanson, S. M., & Weiss, D. S.
772 (2020). DrpB (YedR) Is a Nonessential Cell Division Protein in Escherichia coli. *Journal*
773 *of Bacteriology*, *202*(23), e00284-20. https://doi.org/10.1128/JB.00284-20
774 Yanouri, A., Daniel, R. A., Errington, J., & Buchanan, C. E. (1993). Cloning and sequencing of
775 the cell division gene pbpB, which encodes penicillin-binding protein 2B in Bacillus
776 subtilis. *Journal of Bacteriology*, *175*(23), 7604–7616.
777 https://doi.org/10.1128/jb.175.23.7604-7616.1993
778 Zapun, A., Contreras-Martel, C., & Vernet, T. (2008). Penicillin-binding proteins and β-lactam
779 resistance. *FEMS Microbiology Reviews*, *32*(2), 361–385. https://doi.org/10.1111/j.1574-
780 6976.2007.00095.x
781